Structural basis for ESCRT-III CHMP3 recruitment of AMSH

Supplementary Information

Figure S1: ITC, SPR and pull down data on AMSH interaction with CHMP3ΔN; CHMP1A and CHMP1B (related to Figure 2A) **Figure S2:** Circular dichroism analysis of CHMP3 (related to Figure 1B) **Figure S3:** Cellular localization of GFP-AMSH mutants (related to Figure 2). **Figure S4:** Recombinant AMSH produced as MBP-fusion and without N-terminal tag (related to Figure 5A)

Supplementary methods Pull down. The same concentrations of wild type AMSHΔC (N-terminally His-tagged) and mutants of AMSHΔC were mixed with CHMP3 (no tag) in buffer A and Ni^{2+}-sepharose beads. The mixtures were washed tree times with buffer D (50 mM Tris pH8.5, 500 mM Nacl, 10mM imidazole) and the bound protein fraction was eluted with SDS-loading buffer. For the GST-CHMP1B pull down, equal amounts of either wild type HisAMSHΔC, His-AMSHΔC-K88A and His-AMSHΔC-E104A were mixed with GSTCHMP1B in buffer A (plus 0.25% CHAPS), incubated with Ni^{2+}-sepharose beads and washed three times in buffer E (50mM Tris pH8.5, 500mM Nacl, 10 mM imidazole, 0.5% CHAPS) prior to elution in SDS loading buffer. Samples were separated on a 15% Tris-Tricine gel and bands were visualized with Coomasie brilliant blue. **Circular dichroism.** CD spectroscopy measurements were performed using a JASCO spectropolarimeter equipped with a thermoelectric temperature controller. Spectra of each sample were recorded at 20 ºC in buffer E (20 mM phosphate, pH 7, 100 mM NaCl). For thermal denaturation experiments, the ellipticity was recorded at 222 nm with 1 ºC steps from 20 to 90 ºC with a slope of 1º/min. Ellipticity values were converted to mean residue ellipticity. The helical content was calculated using the program K2d (http://www.embl.de/~andrade/k2d/).

Isothermal titration calorimetry. Calorimetric measurements were carried out using a VP-ITC instrument with a cell volume of 1.4569 ml (MicroCal, LLC). MBP-AMSH(1206) and His-MBP-CHMP3ΔN were exchanged into a buffer containing 20 mM Hepes pH 8.0, 100 mM NaCl. MBP-AMSH(1-206) was used at a concentration of 15 µM in the cell and His-MBP-CHMP3ΔN was injected at a concentration of 150 µM. Interaction constants characterizing the AMSH and CHMP3 interaction were determined by titration at 25°C. The solution in the cell was stirred at 286 rpm to ensure rapid mixing. The interaction isotherms were analyzed using the Origin software package supplied by MicroCal. An interaction model assuming *n* independent and equivalent binding sites was applied, and the stoichiometry *n*, change in enthalpy ΔH^{0} and binding constant K_D were iteratively fitted. **Surface plasmon resonance.** All experiments were performed in duplicate with a Biacore X instrument (Biacore *Inc*.) at 25ºC in a buffer containing 20 mM HEPES pH 7.4, 150 mM NaCl, 50 µM EDTA, 0.005% Surfactant P20 at a flow rate of 20 µl/min. His-MBP-CHMP3ΔN was immobilized on channel 2 of an NTA chip at a concentration of 5.4 µg/ml for 2 min, channel 1 was used as control. MBP-AMSHΔC was passed over the chip surface at concentrations of 1000, 400, 200, 100 and 50 nM for 3 min and dissociation was recorded for 10 min. Afterwards, the chip was regenerated with 0.35 M EDTA in Hepes buffer for 1 min at a flow rate of 50 µl/min and 100 mM NaOH, respectively, followed by recharging with 500 µM $NiCl_2$ in Hepes buffer for 2 min at 30 µl/min. For the analyses of CHMP1A/B interaction with AMSH, a CM5 chip was coated with ant-GST antibodies and GST-CHMP1A or B were bound on channel 2 at a concentration of approximately 200RU for 150 seconds, channel 1 was used as control.

MBP-AMSH(1-206) was passed over the chip surface at concentrations of 5000, 2000, 1000, 500 and 350nM for GST-CHMP1A and 5000, 3000,1500, 1000 and 500nM for GST-CHMP1B for 300 secondes and dissociation was recorded for 10 min. The chip was regenerated with 10mM glycine pH 2.5 for 150 seconds at a flow rate of 50 µl/min.

For the analyses of the AMSHΔC mutants, a CM5 chip was coated with CHMP3 and the analytes, His-AMSHΔC and the His-AMSHΔC mutants were passed over the chip surface at concentrations ranging from 17 to 100 nM (His-AMSHΔC), 0.25 to 4 uM (K88A mutant) and 152 to 1140 nM (E104A mutant). Binding kinetics was evaluated using the BiaEvaluation software package (BIAcore, Inc.) using a Langmuir model 1:1 with no mass transfer.

Supplementary figures:

Figure S1. AMSH interaction with CHMP3ΔN. Related to Figure 2A

(A) Isothermal titration calorimetric data recorded upon injection of MBP-CHMP3ΔN into the cell containing MBP-AMSH(1-206).

(B) The binding curve fitted to a 1:1 stoichiometric binding model.

(C) SPR sensorgrams recorded upon injection of MBP-AMSHΔC (residues 1-146) to Ni-NTA immobilized His-MBP-CHMP3ΔN. Concentrations of the analyte were 1000, 400, 200, 100 and 50 nM.

(D) SPR sensorgrams of CHMP1A (upper panel) and CHMP1B (lower panel) binding to MBP-AMSH(1-206). GST-CHMP1A and GST-CHMP1B was captured by an anti-GST antibody coupled to a CM5 chip. The concentrations of the analyte MBP-AMSH(1-206) were 5000, 2000, 1000, 500 and 350 nM for GST-CHMP1A and 5000, 3000,1500, 1000 and 500 nM for GST-CHMP1B.

(E) Pull down of GST-CHMP1B by His-AMSHΔC wild type, K88A and E104A mutants.

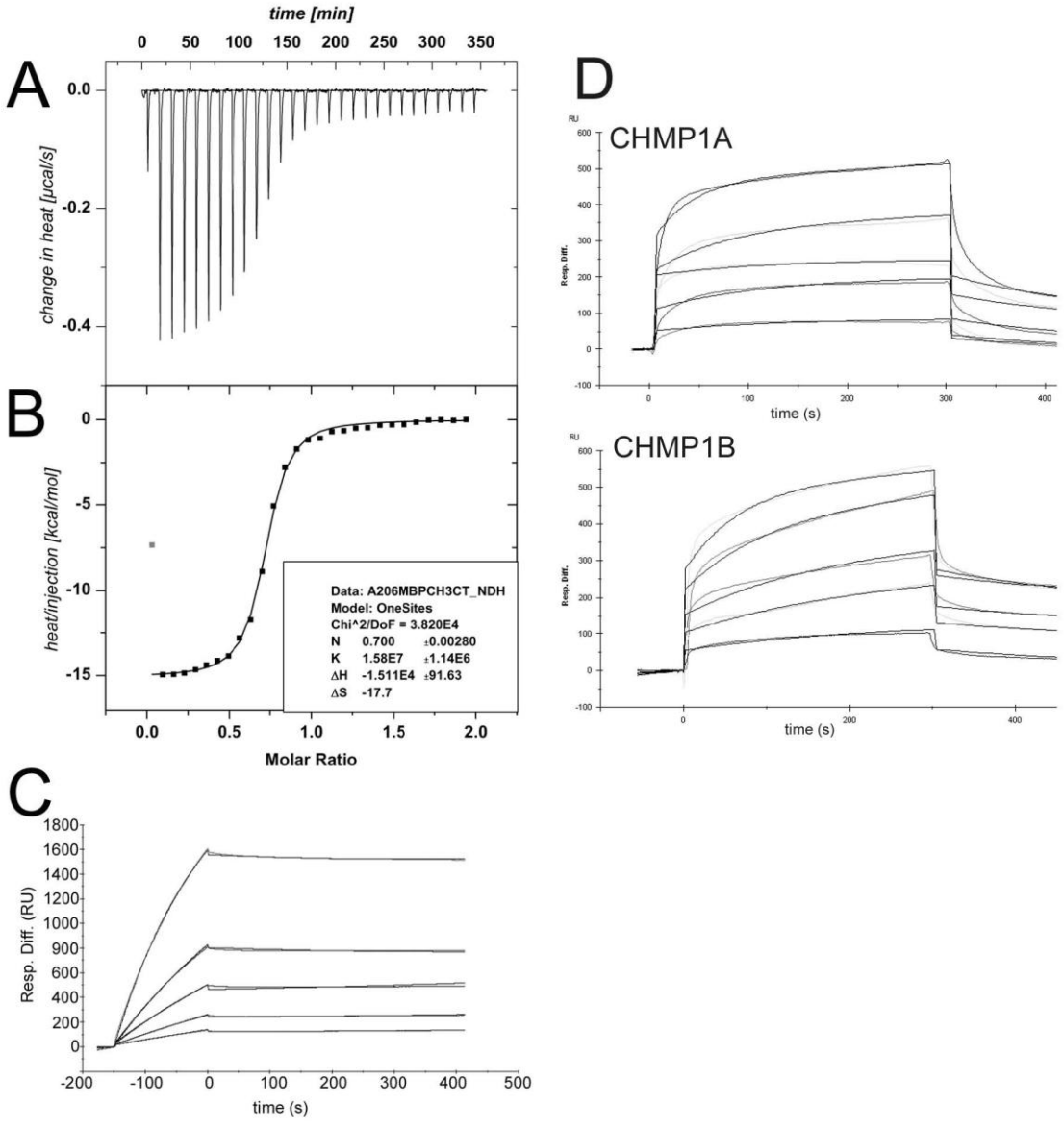
A
time [min]
0 50 100 150 200 250 300 350
0.0
-0.2
-0.4
change in heat [µcal/s]
B
0
-5
-10
-15
heat/injection [kcal/mol]
Data: A206MBPCH3CT_NDH
Model: OneSites
Chi^2/DoF = 3.820E4
N 0.700 ±0.00280
K 1.58E7 ±1.14E6
ΔH -1.511E4 ±91.63
ΔS -17.7
0.0 0.5 1.0 1.5 2.0
Molar Ratio
C
Resp. Diff. (RU)
1800 1600 1400 1200 1000 900 600 400 200 0
-200 -100 0 100 200 300 400 500
time (s)
D
CHMP1A
RU
Resp. Diff.
600 500 400 300 200 100 0 -100
0 100 200 300 400
time (s)
CHMP1B
RU
Resp. Diff.
600 500 400 300 200 100 0 -100
0 200 400
time (s)

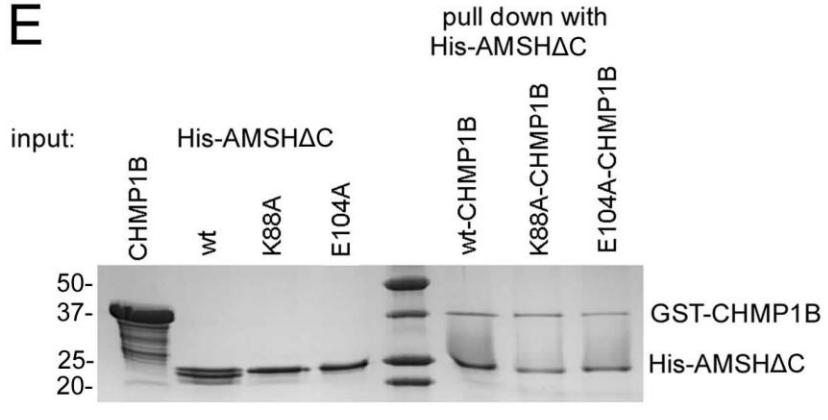
E
pull down with
His-AMSHΔC
input:
His-AMSHΔC
CHMP1B
wt
K88A
E104A
wt-CHMP1B
K88A-CHMP1B
E104A-CHMP1B
50-
37-
25-
20-
GST-CHMP1B
His-AMSHΔC

Figure S2. Circular dichroism analysis of CHMP3. Related to Figure 1B.

(A) Spectrum of CHMP3ΔN (residues 183-222) typical for a random coil structure.

(B) Spectra of CHMP3 and CHMP3(9-183). The calculated helical content of CHMP3 is 60%, corresponding to ~ 133 residues. The spectrum of CHMP3(9-183) results in 68% helicity, which corresponds to ~ 119 residues, consistent with the crystal structure of CHMP3(9-183) with ~117 residues in a helical conformation.

(C) Both CHMP3 and CHMP3(9-183) show melting temperatures of ~ 60 ºC, indicating that the C-terminus does not contribute to the stability of CHMP3.

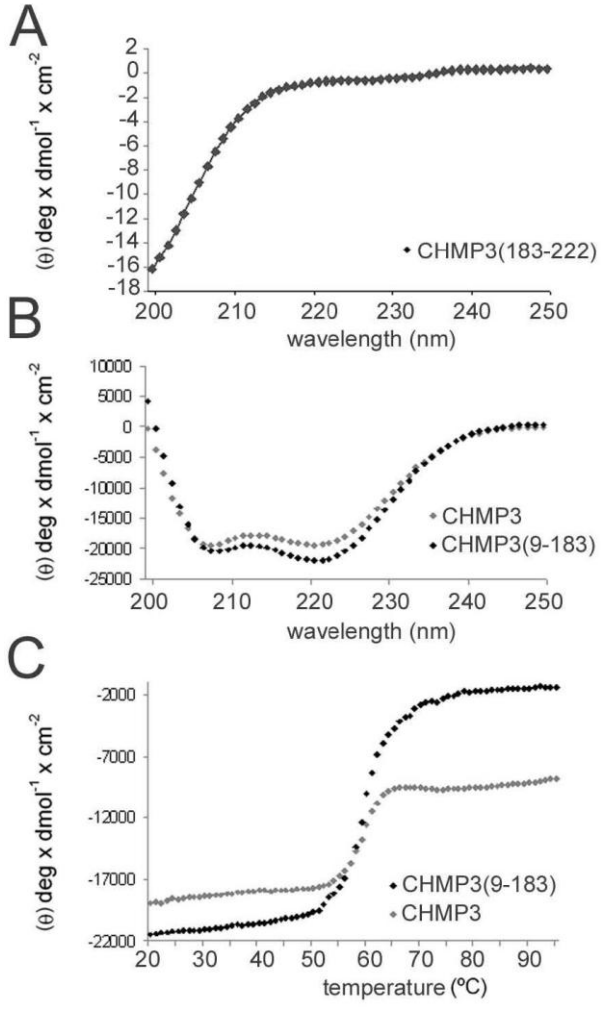

Figure S3. Cellular localization of GFP-AMSH mutants. Related to Figure 2.

The CHMP3 binding mutants of AMSH, GFP-AMSH(D348A-K88A), GFP-AMSH(D348A-E104A) and GFPAMSH(D348A-K107A) show the same cellular localization as the catalytically inactive wild type GFP-AMSH(D348A).

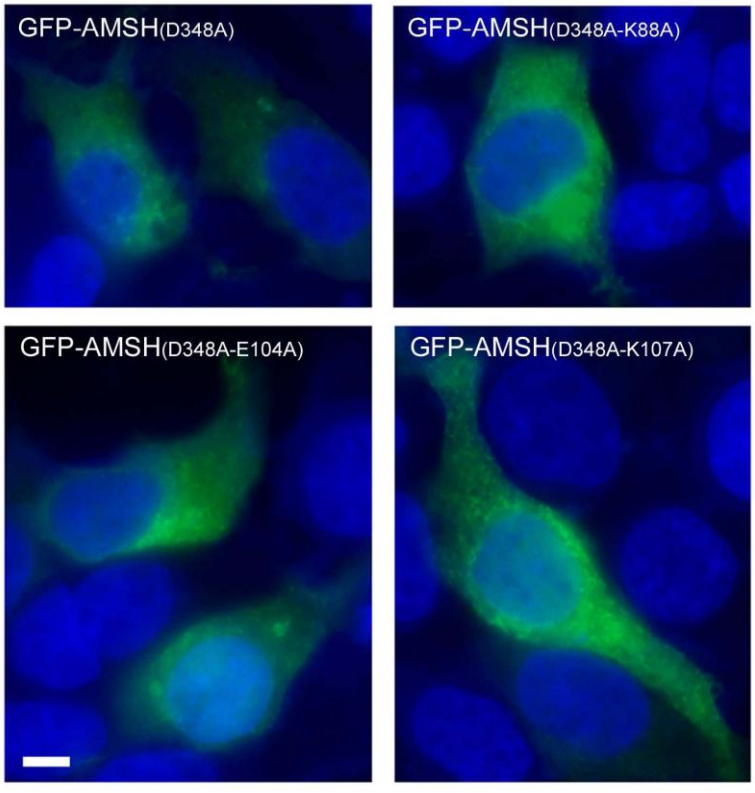

Figure S4: Recombinant AMSH produced as MBP-fusion and without N-terminal. Related to Figure 5A.

(A) The S200 gel filtration profile of MBP-AMSH and SDS-PAGE analysis of corresponding fractions show that MBP-AMSH elutes from ~ 7.5 ml to 14.5 ml in three different peaks that represent aggregates, oligomers and monomers (arrow).

(B) AMSH purified without tag elutes as a single peak from a superdex 20 gel filtration column.